Indirect Determination of Self-Exchange Electron Transfer Rate Constants

Stephen F. Nelsen,*,† Rustem F. Ismagilov,† Kevin E. Gentile,† Mark A. Nagy,† Hieu Q. Tran,† Qinling Qu,‡ DeWayne T. Halfen,‡ Amy L. Odegard,‡ and Jack R. Pladziewicz*,‡

Contribution from the Department of Chemistry, University of Wisconsin, Madison, Wisconsin 53706-1396, and Department of Chemistry, University of Wisconsin, Eau Claire, Wisconsin 54702

Received March 31, 1998

Abstract: Second-order rate constants k_{ij}(obsd) measured at 25 °C in acetonitrile by stopped-flow spectrophotometry for forty-four electron transfer (ET) reactions among fourteen 0/+1 couples [three aromatic compounds (tetrathiafulvalene, tetramethyltetraselenafulvalene, and 9,10-dimethyl-9,10-dihydrophenazine), four 2,3-disubstituted 2,3-diazabicyclo[2.2.2]octane derivatives, six acyclic hydrazines, and the bridgehead diamine 1,5-diazabicyclo[3.3.3]undecane] and seventeen compounds and forty-seven reactions from a previous study (*J. Am. Chem. Soc.* **1997**, *119*, 5900) [three *p*-phenylenediamine derivatives, four ferrocene derivatives, and ten tetraalkylhydrazines] are discussed. When all 91 k_{ij}(obsd) values are simultaneously fitted to Marcus's adiabatic cross rate formula k_{ij}(calcd) = $(k_{ii}k_{jj}K_{ij}f_{ij})^{1/2}$, ln f_{ij} = $(\ln K_{ij})^2/4 \ln(k_{ii}k_{jj}/Z^2)$, best-fit self-exchange rate constants, k_{ii}(fit), are obtained that allow remarkably accurate calculation of k_{ij}(obsd); k_{ij}(obsd)/k_{ij}(calcd) is in the range 0.5−2.0 for all 91 reactions. The average difference without regard to sign, $|\Delta\Delta G^{\ddagger}_{ij}|$, between observed cross reaction activation free energy and that calculated using the k_{ii}(fit) values and equilibrium constants is 0.13 kcal/mol. The $\Delta G^{\ddagger}_{ii}$(fit) values obtained range from 2.3 kcal/mol for tetramethyltetraselenafulvalene$^{0/+}$ to 21.8 kcal/mol for tetra-*n*-propylhydrazine$^{0/+}$, corresponding to a factor of 2×10^{14} in k_{ii}(fit). The principal factor affecting k_{ii}(fit) for our data appears to be the internal vertical reorganization energy (λ_v), but k_{ii}(fit) values also incorporate the effects of changes in the electronic matrix coupling element (V). Significantly smaller V values for ferrocenes and for hydrazines with alkyl groups larger than methyl than for aromatics and tetramethylhydrazine are implied by the observed $\Delta G^{\ddagger}_{ii}$(fit) values.

Introduction

Study of outer-sphere single electron transfer (ET) reactions between a neutral species $\mathbf{i^0}$, and a radical cation, $\mathbf{j}^+$, eq 1, makes

$$\mathbf{i^0} + \mathbf{j}^+ \rightarrow \mathbf{i}^+ + \mathbf{j^0} \quad (1)$$

inclusion of corrections for electrostatic work terms unnecessary, and Marcus's cross reaction relationship simplifies to eq 2.[1] K_{ij}

$$k_{ij}(\text{calcd}) = (k_{ii}k_{jj}K_{ij}f_{ij})^{1/2} \quad (2a)$$

$$\ln(f_{ij}) = [\ln(k_{ij})]^2/[4 \ln(k_{ii}k_{jj}/Z^2)] \quad (2b)$$

and k_{ij} are the equilibrium constant and cross reaction rate constant for eq 1, k_{ii} and k_{jj} are the self-exchange ET rate constants, and Z is the preexponential factor. The more general form of eq 2, including work terms, has been successfully applied to a wide variety of inorganic, organic, organometallic, and biochemical reactions.[2−4]

We recently reported a study of forty-seven such reactions (at 25 °C, in acetonitrile containing 0.1 M tetrabutylammonium perchlorate) between ten tetra-α-branched alkylhydrazines, four ferrocene derivatives, and three *p*-phenylenediamine derivatives.[5] All 17 of these couples have isolable neutral and radical cation oxidation states. Their formal redox potentials ($E^{\circ\prime}$) were measured under the same conditions against a common reference, making ΔG° for their cross reactions known to ±0.2 kcal/mol. A significant advantage of cross reaction studies is that because k_{ij} is sensitive to ΔG° and the average k_{ii}, the same method may be used to study couples that have a wide range of k_{ii} values. A least-squares regression of the 47 observed cross reaction rate constants, k_{ij}(obsd), to eq 2 using $Z = 1 \times 10^{11}$ M^{-1} s^{-1} produced fitted self-exchange rate constants, k_{ii}(fit), for these couples that allowed quite accurate calculation of the cross reaction rate constants, k_{ij}(calcd): k_{ij}(obsd)/k_{ij}(calcd) ratios were in the range 0.5−2 for all reactions, and the average energy barrier difference without regard to sign, $|\Delta\Delta G^{\ddagger}_{ij}|$, between the observed cross reaction activation free energy and that calculated from the k_{ii}(fit) and K_{ij} values was 0.13 kcal/mol. Furthermore, self-ET rate constants directly measured by magnetic resonance line broadening techniques, k_{ii}(MR), are available for 11 of these compounds, allowing a direct evaluation of the accuracy of eq 2 for many of the reactions. The k_{ii}(fit) values were in rather good agreement with the directly measured k_{ii}(MR) values,

† Madison.

‡ Eau Claire.

(1) (a) Marcus, R. A. *J. Chem. Phys.* **1956**, *24*, 966. (b) Marcus, R. A. *Discuss. Faraday Soc.* **1960**, *29*, 21. (c) Marcus, R. A. *J. Phys. Chem.* **1963**, *67*, 853, 2889. (d) Marcus, R. A.; Sutin, N. *Inorg. Chem.* **1975**, *14*, 213.

(2) (a) Marcus, R. A.; Sutin, N. *Biochim. Biophys. Acta* **1985**, *811*, 265. (b) Sutin, N. *Prog. Inorg. Chem.* **1983**, *30*, 441.

(3) Wherland, S. *Coord. Chem. Rev.* **1993**, *123*, 169−99.

(4) Eberson, L. *Electron-Transfer Reactions in Organic Chemistry*, Springer-Verlag: Heidelberg, 1987.

(5) Nelsen, S. F.; Ramm, M. T.; Ismagilov, R. F.; Nagy, M. A.; Trieber, D. A., II.; Powell, D. R.; Chen, X.; Gengler, J. J.; Qu, Q.; Brandt, J. L.; Pladziewicz, J. R. *J. Am. Chem. Soc.* **1997**, *119*, 5900.

S0002-7863(98)01089-0 CCC: $15.00
Published on Web 07/29/1998

although systematically low by a small amount, with the average $\Delta\Delta G^{\ddagger}_{ii} = \Delta G^{\ddagger}_{ii}(\text{fit}) - \Delta G^{\ddagger}_{ii}(\text{MR})$ of 0.64 kcal/mol. The effectiveness of eq 2 in correlating reactions for such a wide variety of compounds is somewhat surprising because as discussed in detail below, the preexponential factor should vary for the different classes of couples studied. Nonetheless, eq 2 correlates all of the reactions remarkably well. Simulations using vibronic coupling ET theory with ET parameters that mimick the k_{ii}(fit) values for hydrazines, ferrocenes, and tetramethyl-*p*-phenylenediamine (**TMPD**) were used to rationalize the good fit to eq 2 despite these differences.

It was concluded that using eq 2 and the approach just described is an effective way to make accurate estimates of k_{ii} for chemical systems for which direct measurement is not presently feasible. This includes three classes of compounds: (1) compounds with k_{ii} values that fall below the minimum accurately determinable by self-ET magnetic resonance line broadening techniques ($k_{ii} \approx 10^3$ M^{-1} s^{-1}) but too large for classical isotopic exchange studies, including many of the hydrazines studied here; (2) compounds of insufficient stability in one oxidation state for direct ET exchange studies, including the acyclic hydrazines used in this study; and (3) compounds with very large k_{ii} that approach the diffusion limit, including the aromatic compounds studied here. While dynamic ESR is excellent for determining fast electron exchange rate constants, the extraction of true k_{ii} values from exchange reactions that have rate constants approaching the diffusion limit has two related problems. First, the reactions become partially diffusion limited, and it is the rate constant for the activated ET process which is needed for comparison with slower ET couples. The equation employed to extract k_{ii} uses the solvent viscosity (η): $k_{ii}^{-1} = k_{ii}(\text{obsd})^{-1} - 3\eta/8RT$.[2,7] This may not be quantitatively correct because η is a bulk solvent property and electron exchange occurs between molecules. Second, the reaction rates sometimes become limited by solvent tumbling rates, which also correlate at least roughly with solvent viscosity. This makes k_{ii} values for couples showing "solvent friction" effects not directly comparable with those that do not. Since the stopped-flow k_{ij}(obsd) values ($< 2 \times 10^7$ M^{-1} s^{-1} in the present data set) are far below the rate of diffusion (ca. 1.2×10^{10} M^{-1} s^{-1} in acetonitrile at 25 °C), neither problem occurs when large and small k_{ii} compounds are paired in a cross rate study.

The present work addresses four new issues by studying the compounds shown in Scheme 1: (1) Three aromatic compounds (**TMTSF**, **TTF**, and **DMP**) that have large enough k_{ii} values to have the problems just described have been studied. By matching them with compounds having low k_{ii} and the appropriate reduction potential, it is possible to get useful estimates of their thermally activated k_{ii} values. Attempts to include the additional aromatic compounds, thianthrene and *N*-methylphenothiazine failed owing to their higher formal potentials and consequently immeasurably fast cross reactions with all members of our current data. (2) Four N,N′-bicyclic hydrazines are included because hydrazines having these substitution patterns are the charge-bearing units of dimeric radical cations for which λ has been determined using optical methods,[8] and we hoped to compare $\Delta G^{\ddagger}_{ii}$ with their optically determined λ. (3) Essentially no effects attributable to rate slowing because of steric hindrance of approach of the reactants were found in the previous study,[5] but all of the hydrazines used were tetra-α-branched and had considerable hindrance to approach to their nitrogens. Therefore, the unbranched tetramethyl-, tetraethyl-, tetra-*n*-propyl-, and tetra-*n*-hexylhydrazine as well as both diisopropyldimethylhydrazines are included in this work to examine the result of lowering steric hindrance. (4) Alder's triply trimethylene bridged diamine,[9] **N[333]N**, has been included. This introduces a new structural class to the data set. This diamine is expected to have significant internal vibrational reorganization energy (λ_v) because of a great difference in bonding at the nitrogens' neutral and radical cation oxidation states. The neutral compound has an antibonding interaction between the nitrogen lone pairs, but the radical cation has a "three electron σ-bond"; that is, the odd electron is in the σ^* orbital of a NN bond.[9]

Scheme 1. Additional Redox Couples Used in This Work

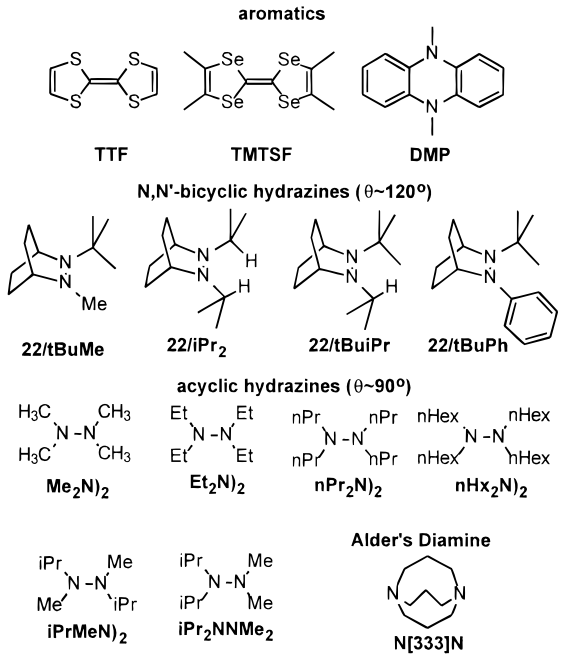

Results

All the reactions reported here were studied by stopped-flow spectrophotometry at 25 °C in acetonitrile with ionic strength maintained with 0.1 M tetrabutylammonium perchlorate and observed to be first order in concentration of both neutral and radical cation components, so that the applicable rate law is given by eq 3. **N** and $\mathbf{R}^{\bullet+}$ are the neutral molecule and radical

$$-\mathrm{d}[\mathbf{R}^{\bullet+}]/\mathrm{d}t = k_{ij}(\text{obsd})[\mathbf{N}][\mathbf{R}^{\bullet+}] \qquad (3)$$

cation used. The reactions were generally studied with **N** in pseudo-first-order excess of $\mathbf{R}^{\bullet+}$ because the neutrals are more stable than their related radical cations and also absorb less in the spectral region used for stopped-flow studies, reducing background absorbance. The first-order dependence of the reaction rate on $[\mathbf{R}^{\bullet+}]$ was established by the observed single

(6) Nelsen, S. F.; Wang, Y. *J. Org. Chem.* **1994**, *59*, 1655.

(7) (a) Grampp, G.; Jaenicke, W. *Ber. Bunsen-Ges. Phys. Chem.* **1984**, *88*, 325. (b) Grampp, G.; Jaenicke, W. *Ibid.* **1984**, *88*, 335. (c) Grampp, G.; Jaenicke, W. *Ibid.* **1991**, *95*, 904.

(8) (a) Nelsen, S. F.; Chang, H.; Wolff, J. J.; Adamus, J. *J. Am. Chem. Soc.* **1993**, *115*, 12276. (b) Nelsen, S. F.; Adamus, J.; Wolff, J. J. *J. Am. Chem. Soc.* **1994**, *116*, 1589. (c) Nelsen, S. F.; Ramm, M. T.; Wolff, J. J.; Powell, D. R. *J. Am. Chem. Soc.* **1997**, *119*, 6863. (d) Nelsen, S. F.; Ismagilov, R. F.; Powell, D. R. *J. Am. Chem. Soc.* **1996**, *118*, 6313. (e) Nelsen, S. F.; Ismagilov, R. F.; Powell, D. R. *J. Am. Chem. Soc.* **1997**, *119*, 10213.

(9) (a) Alder, R. W. *Acc. Chem. Res.* **1983**, *16*, 321. (b) Alder, R. W. *Tetrahedron* **1990**, *46*, 687. (c) Alder, R. W.; Sessions, R. B. In *The Chemistry of Amino, Nitroso, and Nitro Compounds and their Derivatives*; Patai, S., Ed.; Wiley: New York, 1982; Chapter 18, p 763.

Scheme 2. Redox Couples Previously Used

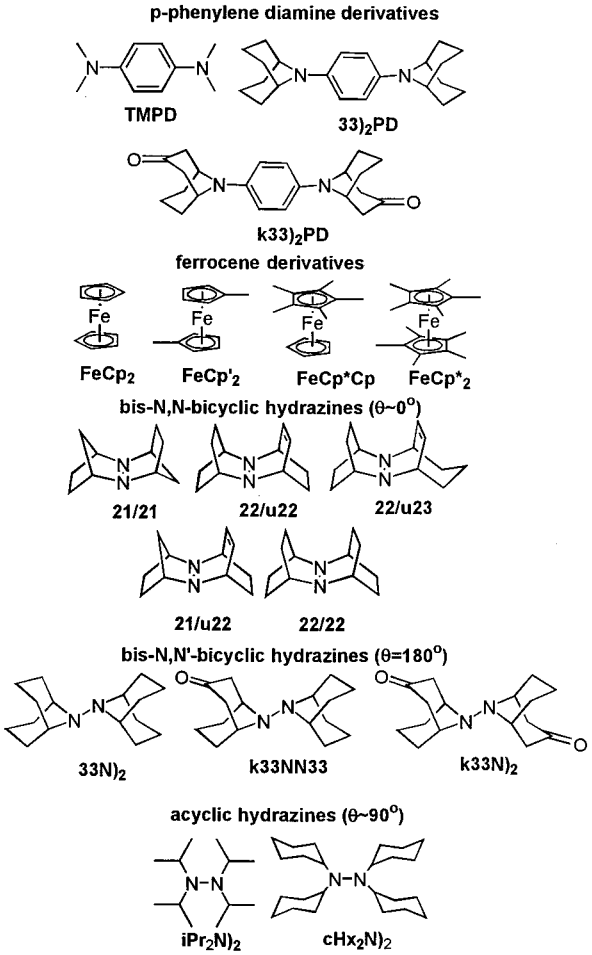

exponential dependence of the absorbance change with time. The first-order dependence of the reaction rate on [**N**] was established by the linearity of plots of the observed first-order rate constants versus [**N**]. Reactions were typically studied over a 10-fold or greater range of [**N**], and k_{ij}(obsd) values were obtained from slopes of these plots. The neutral (reduced) forms of the additional ET couples studied in this work are shown in Scheme 1, and those that were in the previous 47 reaction set in Scheme 2. The $E^{\circ\prime}$ values for all 31 couples are in Table 1.

The radical cations of hydrazines containing alkyl groups that are not α-branched cannot be isolated because their N*CH* bonds are too labile, but the neutral compounds are stable and can serve as the reductant in cross reactions. Consequently, k_{ij}(obsd) could be measured for reactions including **22/tBuMe**^{0} or **N-[333]N**^{0} despite the presence of relatively acidic hydrogens in their radical cations. However, significant deviations from pseudo-first-order behavior are observed for tetra-*n*-alkylhydrazines, e.g., **nPr$_2$N)$_2$**, when studied with most of the oxidants previously employed. Long reaction times are typically required for these reactions because k_{ii} values for tetra-*n*-alkylhydrazines are small. During longer reactions the radical cations become deprotonated to α-hydrazinyl radicals by the excess of basic hydrazine present. These radicals are powerful reductants and react with extra oxidant, causing significant deviations from pseudo-first-order kinetics even in the presence of a large excess of reductant. This problem is avoided by using the large k_{ii} aromatic compounds **TMTSF**$^+$, **TTF**$^+$, and **k33)$_2$PD**$^+$ as oxidants, making their cross reactions fast enough that radical cation decomposition no longer competes with the cross reaction and good pseudo-first-order kinetics over a range of hydrazine concentrations are obtained.

The 44 cross reactions studied and their observed second-order rate constants are summarized in Table 2. These 44 rate constants were combined with 47 previously reported[5] to create a database of 91 cross reactions of 31 compounds for analysis using eq 4. Equation 4 is obtained by rearranging eq 2. The

$$\ln k_{ii} + \ln k_{jj} = A_{ij} \tag{4a}$$

$$A_{ij} = (\ln k_{ij} - 0.5 \ln K_{ij} + \ln Z) - [(\ln Z - \ln k_{ij})^2 + \ln K_{ij}(\ln Z - \ln k_{ij})]^{1/2} \tag{4b}$$

91 k_{ij}(obsd) values and their equilibrium constants were used to calculate the related A_{ij} values, and these were simultaneously fit to eq 4a using $Z = 1 \times 10^{11}$ M^{-1} s^{-1} to produce the best fit self-exchange rate constants, k_{ii}(fit), that appear in Table 1. A plot of k_{ij}(calcd) versus k_{ij}(obsd) (see Figure 1) demonstrates the ability of eq 2 to estimate k_{ij}(obsd) accurately using these k_{ii}(fit) values. All k_{ij}(calcd)/k_{ij}(obsd) ratios lie between 0.5 and 2.0, and the average $|\Delta\Delta G^{\ddagger}_{ii}|$ remains at 0.13 kcal/mol for the 91 reaction set, corresponding to a change in k_{ij} of ca. 20%.

The k_{ii}(fit) value range is 2×10^{14}, demonstrating the extraordinary range of intrinsic ET reactivity of the compounds employed. Self-exchange activation free energies are used to compare different couples because free energies are linearly related, while rate constants are related exponentially. Moreover, we have chosen to compare $\Delta G^{\ddagger}_{ii}$(fit), obtained from the Eyring equation, $k_{ii}(\text{fit}) = (k_b T/h) \exp[-\Delta G^{\ddagger}_{ii}(\text{fit})/RT]$, rather than classical Marcus activation free energies, ΔG^{*}_{ii}(fit), because the former are more frequently cited for experimentally determined rate constants in the literature, allowing direct comparisons. Because of the difference in preexponential terms between classical Marcus theory and the Eyring equation, $\Delta G^{*}_{ii}(\text{fit}) = \Delta G^{\ddagger}_{ii}(\text{fit}) - 2.45$ kcal/mol at 25 °C and the $\Delta G^{\ddagger}_{ii}$(fit) values given in Table 1 can be readily converted to the classical Marcus activation free energies. Introducing new data can in principle change the values obtained for all couples in the set because a least-squares fit to the entire data set is employed. For this reason, we show the number of reactions involving each partner and $\Delta G^{\ddagger}_{ii}$ value from the 47 reaction data set[5] in parentheses after the entries for the present, 91 reaction data set. Changes in $\Delta G^{\ddagger}_{ii}$(fit) from those of the 47 reaction set are small (≤0.1 kcal/mol) for all of the 17 couples except **FeCp′$_2$**$^{0/+}$, where the change is 0.3 kcal/mol. This gives confidence that the $\Delta G^{\ddagger}_{ii}$(fit) values obtained are reasonably stable, and that their sizes are worth understanding. The **FeCp′$_2$**$^{0/+}$ couple was only included in one reaction in the 47 reaction set, so the least-squares fitting procedure assigns k_{ii}(fit) for **FeCp′$_2$**$^{0/+}$ as that which makes the deviation in k_{ij}(calcd) for this single reaction zero, and is unable to use any averaging. This makes $\Delta G^{\ddagger}_{ii}$(fit) less accurate than for couples used in several reactions. Although **FeCp′$_2$**$^{0/+}$ only appears twice in the larger data set, the new $\Delta G^{\ddagger}_{ii}$(fit) value is between those of its pentamethyl and unmethylated analogues. This is much more reasonable than the dimethyl compound having larger $\Delta G^{\ddagger}_{ii}$(fit) than the more and less highly methylated compounds, as it was assigned in the 47 reaction set.

The $\Delta G^{\ddagger}_{ii}$(fit) values fall into three distinct groups for couples having different structures (see Figure 2), 2.3−7.1 kcal/mol for the aromatics, 7.9−8.2 kcal/mol for the ferrocenes, and the broad range of 12.8−21.8 kcal/mol for the hydrazines. The $\Delta G^{\ddagger}_{ii}$(fit) values for hydrazines also fall into structurally related

Table 1. Data for 31 Redox Couples Obtained Using 91 Cross Reactions

redox couple	$E^{\circ\prime}$, V vs SCE	reactions[a,b]	k_{ii}(fit), M^{-1} s^{-1}	$\Delta G^{\ddagger}_{ii}$(fit),[b] kcal/mol	r,[c] Å	AM1 ΔH_v[d]
			Aromatic Compounds			
TMTSF$^{0/+}$	+0.42	8	1.4×10^{11}	2.3	3.65	
TTF$^{0/+}$	+0.33	9	6.6×10^{9}	4.1	3.12	1.73
DMP$^{0/+}$	+0.14	6	7.4×10^{8}	5.4	3.44	3.88
TMPD$^{0/+}$	+0.12	6 (4)	1.3×10^{8}	6.4 (6.4)	3.25	4.67
33)$_2$PD$^{0/+}$	+0.02	3 (3)	1.7×10^{8}	6.2 (6.2)	4.02	5.27
k33)$_2$PD$^{0/+}$	+0.29	10 (3)	4.1×10^{7}	7.1 (7.1)		
			Ferrocene Derivatives			
FeCp*$_2$ $^{0/+}$	−0.11	8 (6)	1.0×10^{7}	7.9 (7.9)	3.07	
FeCp*Cp$^{0/+}$	+0.12	10 (6)	1.0×10^{7}	7.9 (7.9)		
FeCp′$_2$ $^{0/+}$	+0.28	2 (1)	8.9×10^{6}	8.0 (7.7)		
FeCp$_2$ $^{0/+}$	+0.395	1 (1)	6.5×10^{6}	8.2 (8.1)		
			Bisbicyclic Hydrazines			
21/21$^{0/+}$	+0.01	4 (4)	2.7×10^{3}	12.8 (12.7)	3.13	8.81
22/u22$^{0/+}$	−0.24	5 (4)	1.3×10^{3}	13.1 (13.1)	3.33	9.14
22/u23$^{0/+}$	−0.30	3 (3)	2.5×10^{3}	12.8 (12.8)		
21/u22$^{0/+}$	+0.06	9 (7)	9.2×10^{2}	13.4 (13.4)	3.25	9.72
22/22$^{0/+}$	−0.53	2 (2)	1.1×10^{2}	14.7 (14.7)	3.36	
33N)$_2$ $^{0/+}$	−0.01	10 (8)	7.2×10^{2}	13.6 (13.6)	3.71	9.05
k33NN33$^{0/+}$	+0.22	11 (8)	2.6×10^{2}	14.2 (14.2)		
k33N)$_2$ $^{0/+}$	+0.45	9 (7)	4.4×10^{1}	15.2 (15.3)		
			Monobicyclic Hydrazines			
22/tBuMe$^{0/+}$	+0.11	3	3.4×10^{1}	15.4	3.38	11.63
22/iPr$_2$ $^{0/+}$	+0.08	1	6.4×10^{1}	15.0		
22/tBuiPr$^{0/+}$	−0.10	3	1.4×10^{1}	15.9	3.56	11.51
22/tBuPh$^{0/+}$	+0.26	5	9.9×10^{2}	13.4	3.68	9.49
			Acyclic Hydrazines			
iPr$_2$N)$_2$ $^{0/+}$	+0.26	17 (14)	2.6×10^{-3}	21.0 (21.0)	3.57	13.88
cHx$_2$N)$_2$ $^{0/+}$	+0.26	16 (13)	2.1×10^{-2}	19.8 (19.7)	4.24	
Me$_2$N)$_2$ $^{0/+}$	+0.33	3	1.6×10^{0}	17.2	2.70	14.63
Et$_2$N)$_2$ $^{0/+}$	+0.29	3	7.3×10^{-4}	21.7	3.19	12.35
nPr$_2$N)$_2$ $^{0/+}$	+0.29	3	6.2×10^{-4}	21.8		
nHx$_2$N)$_2$ $^{0/+}$	+0.29	3	1.5×10^{-3}	21.3	4.38	
iPrMeN)$_2$ $^{0/+}$	+0.29	3	1.2×10^{-2}	20.1		
iPr$_2$NNMe$_2$ $^{0/+}$	+0.29	3	4.5×10^{-3}	20.6		
			Diamine			
N[333]N$^{0/+}$	−0.165	3	4.6×10^{1}	15.2		

[a] Number of reactions studied having this compound as a component (Table 2 and Table 2 of ref 4). [b] Numbers in parentheses refer to the 47 reaction set of ref 4, for comparison. [c] Average radius, from the molecular volume calculated using AM1 or PM3, using volume = $(4/3)\pi(r)^3$. [d] Units, kcal/mol. Calculated by the method of ref 12.

groups. The bicyclic substituted cases, which have substantial lone pair−lone pair interaction in their neutral forms (NN bond twist angle (θ) far from 90°) fall in the range 12.8−15.9 kcal/mol, while the $\theta \approx 90°$ acyclic examples have $\Delta G^{\ddagger}_{ii}$ in the range 19.8−21.8 except for **Me$_2$N)$_2$**$^{0/+}$, which shows an intermediate value. Alder's diamine **N[333]N**$^{0/+}$ has a $\Delta G^{\ddagger}_{ii}$(fit) value within the range for hydrazines. The remainder of this paper is aimed at providing a rational basis for understanding these large variations in $\Delta G^{\ddagger}_{ii}$(fit).

Discussion

Barriers for ET. We have analyzed the k_{ii}(fit) values, obtained by assuming a constant preexponential factor in classical Marcus theory, eq 2, using the Eyring expression for a second-order reaction, $k = K_{as}(6.2 \times 10^{12})\exp(-\Delta G^{\ddagger}/RT)$ M^{-1} s^{-1} at 25 °C, where K_{as} is the association constant for precursor complex formation. Since we have thus far been unable to obtain any experimental evidence for complex formation between the cation radicals and neutral molecules paired in this study, let alone measure K_{as} values for our reactions, we have held K_{as} fixed at 1 M^{-1} for this analysis as is frequently done.[2] Both the preexponential term (PRE) and the exponential term are more complicated using ET theory.[2] We shall discuss these results here only in terms of a "semiclassical" model, which uses eq 5 as the rate equation for self-ET.[10] Four ET parameters

$$k_{ii} = \mathrm{PRE}\exp(-\Delta G^{*}/RT) \tag{5a}$$

$$\mathrm{PRE} = K_{as}k_{el}\nu_v \tag{5b}$$

$$k_{el} = [1 - \exp(-\nu_{el}/2\nu_v)]/[1 - {}^1/_2\exp(-\nu_{el}/2\nu_v)] \tag{5c}$$

control k_{ii}: the vertical vibrational reorganization energy (λ_v), solvent reorganization energy (λ_s), V, and $h\nu_v$. The total reorganization energy λ is the sum of λ_v and λ_s. The nuclear coupling frequency (ν_v) is $(2.998 \times 10^{10})h\nu_v$ cm·s^{-1}, and the electronic coupling frequency (ν_{el}) is $(1.52 \times 10^{14})(V^2/\lambda^{1/2})$ s^{-1} at 25 °C. The Marcus free energy of reaction depends on λ and V as shown in eq 6. The value of k_{ii}(fit) establishes the

$$\Delta G^{*} = \lambda/4 - V + V^2/\lambda \tag{6}$$

(10) (a) Weaver, M. J. *Chem. Rev.* **1992**, *92*, 463. (b) Weaver, M. J.;, McManis, G. E., III. *Acc. Chem. Res.* **1990**, *23*, 294. (c) ν_v is usually written as being weighted by an expression that reduces to about $(\lambda_v/\lambda)^{1/2}$,[2, 10a] The compounds considered include ones with this factor varying from ≥0.95 (acyclic hydrazines) to near zero (ferrocenes and **TMTSF**). A great decrease of PRE (which must be accompanied by a large decrease in λ) required by using a $(\lambda_v/\lambda)^{1/2}$ term appears unreasonable to us. This would reduce $\Delta G^{\ddagger}_{s}$ values even further, and they are already rather small.

Table 2. Summary of Reactions Studied[a]

entry	reductant	oxidant	k_{ij}(obsd), M^{-1} s^{-1}	k_{ij}(calcd), M^{-1} s^{-1}	ratio[b]	$\Delta\Delta G^{\ddagger}_{ij}$, kcal/mol
48	**iPr$_2$N)$_2^0$**	**TTF$^+$**	$1.43(4) \times 10^4$	1.60×10^4	0.89	+0.07
49	**cHx$_2$N)$_2^0$**	**TTF$^+$**	$3.4(3) \times 10^3$	4.63×10^4	0.73	+0.18
50	**TTF^0**	**k33N)$_2^+$**	$5.4(3) \times 10^6$	5.1×10^6	1.05	−0.03
51	**k33)$_2$PD^0**	**k33N)$_2^+$**	$9.8(5) \times 10^5$	7.6×10^5	1.29	−0.15
52	**DMP^0**	**iPr$_2$)N$_2^+$**	$2.0(1) \times 10^4$	1.36×10^4	1.48	−0.23
53	**DMP^0**	**cHx$_2$)N$_2^+$**	$3.3(1) \times 10^4$	3.90×10^4	0.85	−0.10
54	**DMP^0**	**22/tBuPh$^+$**	$8.0(3) \times 10^6$	8.14×10^6	0.98	+0.01
55	**33N)$_2^0$**	**DMP$^+$**	$1.3(4) \times 10^7$	1.09×10^7	1.09	−0.10
56	**21/u22^0**	**DMP$^+$**	$2.8(2) \times 10^6$	3.71×10^6	0.75	+0.17
57	**DMP^0**	**k33NN33$^+$**	$1.86(7) \times 10^6$	2.05×10^6	0.91	+0.06
58	**22/tBuMe^0**	**FeCp′$_2^+$**	$3.2(3) \times 10^5$	4.08×10^5	0.78	+0.14
59	**22/tBuMe^0**	**FeCp*Cp$^+$**	$2.3(3) \times 10^4$	2.44×10^4	0.94	+0.04
60	**22/tBuMe^0**	**TMPD$^+$**	$1.1(1) \times 10^5$	8.10×10^4	1.36	−0.18
61	**22/iPr$_2^0$**	**FeCp*Cp$^+$**	$5.9(6) \times 10^4$	5.90×10^4	1.00	+0.00
62	**22/tBuiPr^0**	**FeCp*Cp$^+$**	$8.1(8) \times 10^5$	6.82×10^5	1.19	−0.10
63	**22/tBuiPr^0**	**FeCp*$_2^+$**	$1.4(3) \times 10^4$	1.00×10^4	1.40	−0.20
64	**22/u22^0**	**22/tBuiPr$^+$**	$1.14(8) \times 10^3$	1.89×10^3	0.60	+0.30
65	**TMPD^0**	**22/tBuPh$^+$**	$4.3(3) \times 10^6$	4.71×10^6	0.91	+0.05
66	**FeCp*Cp^0**	**22/tBuPh$^+$**	$1.31(5) \times 10^6$	1.24×10^6	1.05	−0.03
67	**21/u22^0**	**22/tBuPh$^+$**	$4.6(2) \times 10^4$	3.95×10^4	1.16	−0.09
68	**33N)$_2^0$**	**22/tBuPh$^+$**	$1.02(6) \times 10^5$	1.12×10^5	0.91	+0.05
69	**Me$_2$N)$_2^0$**	**k33)$_2$PD$^+$**	$1.7(1) \times 10^3$	2.78×10^3	0.61	+0.29
70	**Me$_2$N)$_2^0$**	**TTF$^+$**	$1.4(1) \times 10^5$	8.55×10^4	1.64	−0.29
71	**Et$_2$N)$_2^0$**	**k33)$_2$PD$^+$**	$2.1(1) \times 10^2$	1.77×10^2	1.19	+0.10
72	**Et$_2$N)$_2^0$**	**TTF$^+$**	$4.5(2) \times 10^3$	5.34×10^3	0.84	−0.10
73	**nPr$_2$N)$_2^0$**	**k33)$_2$PD$^+$**	$1.49(6) \times 10^2$	1.54×10^2	0.97	+0.02
74	**nPr$_2$N)$_2^0$**	**TTF$^+$**	$4.8(3) \times 10^3$	4.65×10^3	1.03	−0.02
75	**nHx$_2$N)$_2^0$**	**k33)$_2$PD$^+$**	$1.9(1) \times 10^2$	1.94×10^2	0.98	+0.01
76	**nHx$_2$N)$_2^0$**	**TTF$^+$**	$5.95(9) \times 10^3$	5.84×10^3	1.02	−0.01
77	**N[333]N^0**	**k33NN33$^+$**	$1.6(1) \times 10^5$	9.90×10^4	1.62	−0.28
78	**N[333]N^0**	**33N)$_2^+$**	$3.2(3) \times 10^3$	3.31×10^3	0.97	+0.02
79	**N[333]N^0**	**FeCp*$_2^+$**	$4.0(3) \times 10^4$	6.35×10^4	0.63	+0.27
80	**iPr$_2$N)$_2^0$**	**TMTSF$^+$**	$5.2(1) \times 10^5$	3.72×10^5	1.38	−0.19
81	**cHx$_2$N)$_2^0$**	**TMTSF$^+$**	$8.0(5) \times 10^5$	1.01×10^6	0.78	+0.15
82	**Et$_2$N)$_2^0$**	**TMTSF$^+$**	$1.05(7) \times 10^5$	1.20×10^5	0.88	+0.08
83	**nPr$_2$N)$_2^0$**	**TMTSF$^+$**	$1.08(4) \times 10^5$	1.11×10^5	0.98	+0.01
84	**nHx$_2$N)$_2^0$**	**TMTSF$^+$**	$2.5(1) \times 10^5$	1.70×10^5	1.48	−0.27
85	**Me$_2$N)$_2^0$**	**TMTSF$^+$**	$4.1(2) \times 10^6$	2.65×10^6	1.56	−0.26
86	**iPrMeN)$_2^0$**	**TMTSF$^+$**	$2.8(3) \times 10^5$	4.79×10^6	0.58	+0.32
87	**iPrMeN)$_2^0$**	**TTF$^+$**	$1.97(4) \times 10^4$	1.94×10^4	1.01	−0.01
88	**iPrMeN)$_2^0$**	**k33)$_2$PD$^+$**	$1.2(1) \times 10^3$	7.06×10^2	1.70	−0.31
89	**iPr$_2$NNMe$_2^0$**	**TMTSF$^+$**	$2.35(9) \times 10^5$	2.95×10^5	0.80	+0.13
90	**iPr$_2$NNMe$_2^0$**	**TTF$^+$**	$1.22(7) \times 10^4$	1.19×10^4	1.03	−0.01
91	**iPr$_2$NNMe$_2^0$**	**k33)$_2$PD$^+$**	$5.3(2) \times 10^2$	4.32×10^2	1.23	−0.12

[a] Entries 1−47 appear in Table 2 of ref 5. [b] Ratio = k_{ij}(obsd)/k_{ij}(calcd).

product of PRE and exp(−ΔG^*(fit)/RT), but only a maximum ΔG^*(fit) if V is considered to be a variable. The maximum ΔG^*(fit) (ΔG^*_{ad}) is that for a completely adiabatic reaction, obtained when V is large enough that k_{el} is unity. Figure 3 shows values for $\Delta G^{\ddagger}_{ii}$(fit) (on the left margin) and the resulting ΔG^*_{ad} (on the right margin) for several couples using conventional values for $h\nu_v$ of 400 cm^{-1} for the ferrocene, 800 cm^{-1} for the hydrazines, and 1500 cm^{-1} for the aromatic compounds. $\Delta G^*_{ad} - \Delta G^{\ddagger}_{ii}$(fit) increases slightly as the $h\nu_v$ employed increases (0.3 kcal/mol at $h\nu_v$ = 400 cm^{-1}, 0.8 at 800 cm^{-1}, and 1.1 at 1500 cm^{-1}), but the effect is small compared to the wide range of ET barriers. ΔG^*, V value pairs that give k_{ii}(fit) for each compound using eq 5 with K_{as} set at unity are shown as the solid lines. Figure 3 illustrates that ΔG^* values that give k_{ii}(fit) vary over several kcal/mol depending upon the size of V: values of $\Delta G^*_{ad} - \Delta G^*$ (V = 0.01 kcal/mol) using the $h\nu_v$ values quoted above are 5.5−5.6 kcal/mol for the two hydrazines, 4.75 for ferrocene, and 5.4, 4.9, and 3.4 kcal/mol for **TMPD$^{0/+}$**, **TTF$^{0/+}$**, and **TMTSF$^{0/+}$**.

As has been noted previously,[2] the existence of k_{ii}(fit) values that allow calculation of accurate k_{ij} values using eq 2 does not require that the reactions studied are adiabatic, despite this assumption being made in deriving eq 2. However, given the

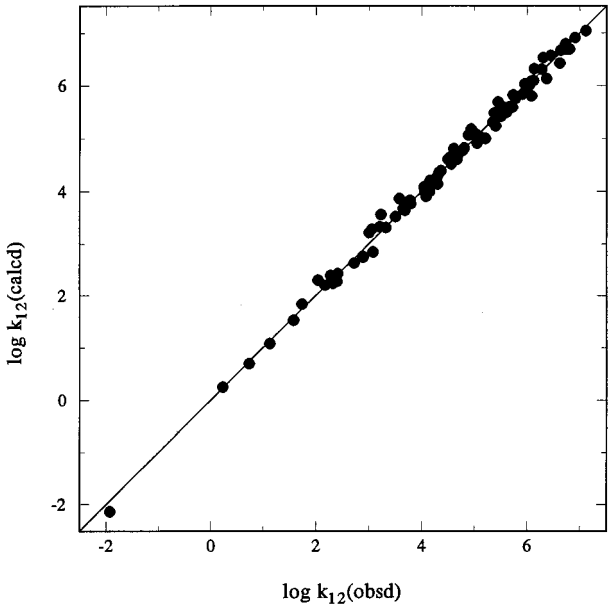

Figure 1. k_{ij}(obsd) versus k_{ij}(calcd) for 91 cross reactions using the k_{ii}(fit) values of Table 1.

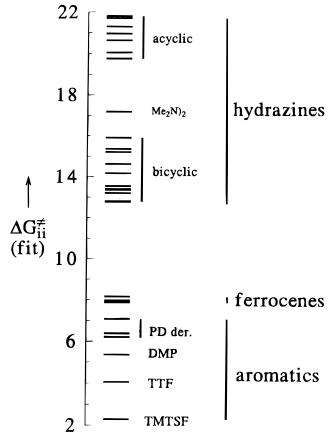

Figure 2. Ranges of $\Delta G^{\ddagger}_{ii}$(fit) values for the aromatics, ferrocenes, and hydrazines studied.

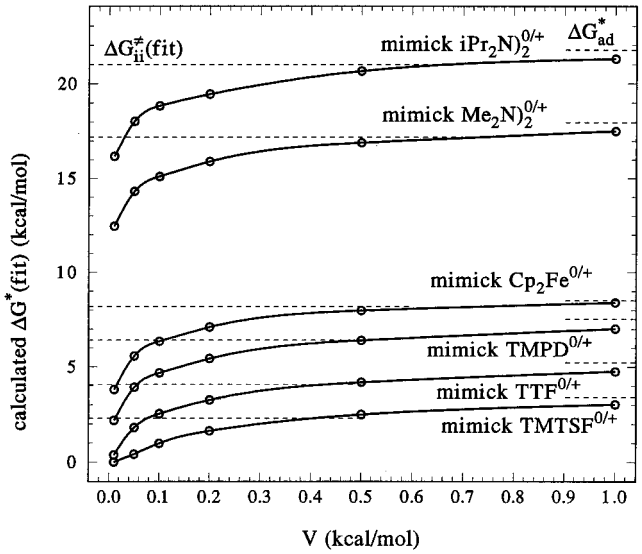

Figure 3. Calculated ΔG^{*}, V pairs that give k_{ii}(fit) values for the hydrazine couples **iPr$_2$N)$_2$**$^{0/+}$ and **Me$_2$N)$_2$**$^{0/+}$ using $h\nu_v = 800$ cm^{-1}, **Cp$_2$Fe**$^{0/+}$ using $h\nu_v = 400$ cm^{-1}, and aromatic couples **TMPD**$^{0/+}$, **TTF**$^{0/+}$, and **TMTSF**$^{0/+}$ using $h\nu_v = 1500$ cm^{-1}. (For simplicity, K_{as} was set equal to 1 to draw these plots.)

likely differences in $h\nu_v$ and V for the range of compounds studied, one might have expected substantial deviations from eq 2 for this extensive data set. While the fit to eq 2 is not perfect, and some individual reactions show significant deviations, we discern no pattern in the deviations and the overall fit is remarkably good, which suggests that the geometric mean averaging of preexponential factors implied by eq 2 ($PRE_{12} \cong ((PRE_{11})(PRE_{22}))^{1/2}$) is adequate. The information available about ET reactions by considering their $\Delta G^{\ddagger}_{ii}$(fit) values will be the focus of the rest of the discussion.

Aromatics. Self-exchange rate constants, k_{ii}, measured using dynamic ESR at 293 K as a function of solvent have been reported by Grampp and Jaenicke for two of the six aromatic compounds studied, **TMPD**$^{0/+}$ and **TTF**$^{0/+}$.[7] Their relative k_{ii} values are very solvent dependent. $\Delta G^{\ddagger}_{ii}$ for **TMPD**$^{0/+}$ depends linearly on the Marcus solvent parameter γ, which depends only upon bulk solvent properties, the refractive index (n) and the static dielectric constant (ϵ_s): $\gamma = n^{-2} - \epsilon_s^{-1}$. In contrast, the k_{ii} values for **TTF**$^{0/+}$ show a significant solvent friction effect, decreasing with increasing solvent viscosity. The ratio k_{ii}(**TTF**$^{0/+}$)/k_{ii}(**TMPD**$^{0/+}$) is about 3.1 in acetone (**TMPD**$^{0/+}$ was not studied in acetone, and we interpolated its k_{ii} value using the γ for acetone), but drops to 0.69 in dimethylformamide and to 0.08 in hexamethylphosphoramide. These data do not allow simple consideration of how the ET parameters for these couples differ.

Table 3. Calculated Contributions to $\Delta G^{\ddagger}_{ii}$(fit) (kcal/mol) from Solvent and Vertical Reorganization Energies

couple	ΔG^{*}_s(calcd)[a]	$\Delta G^{\ddagger}_s$(max)[b]	$\Delta G^{\ddagger}_v$(min)[b]	ΔH_v(calcd)[c] (AM1 [PM3])
TMTSF$^{0/+}$	6.0	[2.3]	[0]	− [0.97]
TTF$^{0/+}$	7.0	2.7	1.4	1.73 [1.63]
DMP$^{0/+}$	6.4	2.4	3.0	3.89 [4.52]
TMPD$^{0/+}$	6.7	2.6	3.8	4.68 [7.24]
33)$_2$PD$^{0/+}$	5.5	2.1	4.1	5.28 [6.75]

[a] Obtained from eq 7. [b] Calculated assuming $\Delta G^{\ddagger}_{ii}$(fit) = $\Delta G^{\ddagger}_s$(**TMTSF**$^{0/+}$), i.e., that $\Delta G^{\ddagger}_v$(**TMTSF**$^{0/+}$) = 0. [c] The value calculated by AM1 (kcal/mol) is followed in brackets by that calculated using PM3.

Since the cross reaction data were obtained under conditions where solvent friction effects are not significant, the $\Delta G^{\ddagger}_{ii}$(fit) values are activation limited even for the lowest barrier couple, **TMTSF**$^{0/+}$. The five aromatic compounds of Table 1 that lack keto substituents (**k33)$_2$PD**$^{0/+}$ is discussed separately later) range over a factor of 1000 in k_{ii}(fit). Table 3 summarizes their analysis in terms of solvent and vibrational reorganization free energies using $\Delta G^{\ddagger}_{ii}$(fit) = $\Delta G^{\ddagger}_s + \Delta G^{\ddagger}_v$. Marcus's dielectric continuum λ_s equation[2] in acetonitrile at 25 °C may be written as eq 7, where r is the average molecular radius (Å), if a distance

$$\Delta G^{*}_s(\text{calcd}) = \lambda_s/4 = 21.92/r \qquad (7)$$

factor of $1/2r$, that expected using the "touching spheres" model of the transition state, is employed. We use r values obtained from the calculated molecular volume using volume = $(4/3)\pi(r)^3$, and list these values in Table 1. Equation 7 ΔG^{*}_s(calcd) values are obviously too large to be $\Delta G^{\ddagger}_s$ values: most exceed $\Delta G^{\ddagger}_{ii}$(fit). Arguments from other results that eq 7 ΔG^{*}_s(calcd) values are too large have been summarized by Formosinho and co-workers.[11] The maximum $\Delta G^{\ddagger}_s$ value that can fit our data for **TMTSF**$^{0/+}$ is that using $\Delta G^{\ddagger}_v = 0$ for this compound. Values of $\Delta G^{\ddagger}_s$(max) obtained using the $1/r$ dependence of eq 7, as well as the related $\Delta G^{\ddagger}_v$(min) values, appear in Table 3. Semiempirical calculations of the enthalpy contribution to λ_v (λ'_v) as previously described[12] were carried out to attempt quantitation of the effect of λ_v variations in this series. The results of both AM1 calculations, previously reported as λ'_v(**TMPD**$^{0/+}$) = 18.7 kcal/mol, and λ'_v(**33)$_2$PD**$^{0/+}$) = 21.1 kcal/mol,[13] and PM3 calculations are listed in Table 3. We lack AM1 parameters for selenium, and can only report the PM3 result for **TMTSF**$^{0/+}$. These semiempirically calculated λ'_s values obviously may not be highly accurate, and the AM1 and PM3 results do not agree very well for the nitrogen-containing compounds. It is nevertheless striking that the $\Delta G^{\ddagger}_v$(min) values estimated assuming $\Delta G^{\ddagger}_v = 0$ for **TMTSF**$^{0/+}$ give a linear plot versus AM1 ΔH_v, extrapolating to $\Delta G^{\ddagger}_v$(min) near 0 at ΔH_v = 0 (see Figure 4). Also shown is the line obtained assuming $\Delta G^{\ddagger}_v = 1$ for **TMTSF**$^{0/+}$. Because it seems very unlikely that $\Delta G^{\ddagger}_s$ for **TMTSF**$^{0/+}$ would be smaller than 1.3 kcal/mol, it

(11) Formosinho, S. J.; Arnaut, L. G.; Fausto, R. *Prog. React. Kinet.*, in press. We thank Professor Arnaut for a reprint.

(12) Nelsen, S. F.; Blackstock, S. C.; Kim, Y. *J. Am. Chem. Soc.* **1987**, *109*, 677.

(13) (a) Nelsen, S. F.; Yunta, M. J. R. *J. Phys. Org. Chem.* **1994**, *7*, 55. (b) As discussed,[9a] λ'_v is very sensitive to twisting at the CN bonds, and AM1 calculations obtain minimum energy structures having twisting at these bonds, we believe incorrectly. The numbers used for **TMPD**$^{0/+}$ and **33)$_2$PD**$^{0/+}$ enforce untwisted structures, which produce the lower values quoted. The PM3 calculations used the AM1 results as input files for geometry optimization with the AM1 keyword replaced by PM3.

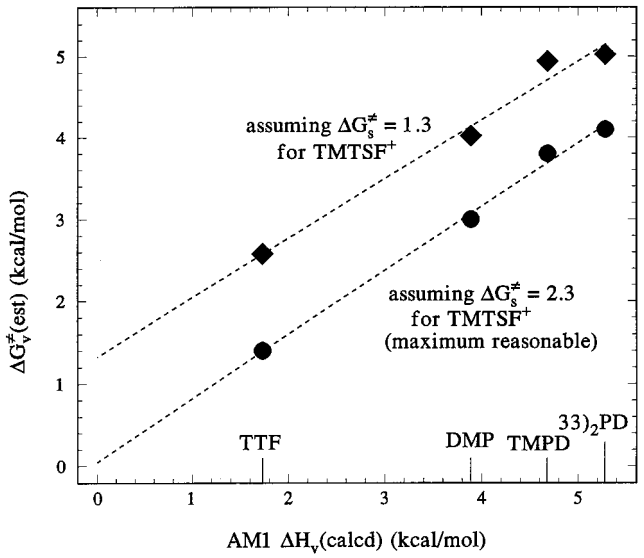

Figure 4. Estimated vertical reorganization energy versus AM1-calculated vertical reorganization energy for five aromatic compounds. The circles shown correspond to the assumption that $\Delta G^{\ddagger}_v$(**TMTSF**$^{0/+}$) is zero, and the squares to the assumption of a value of 1 kcal/mol.

seems unlikely that its $\Delta G^{\ddagger}_v$ could be larger than about 1 kcal/mol, so we suggest that Figure 3 includes the whole range likely for $\Delta G^{\ddagger}_v$ for the aromatic couples plotted. Our kinetic data are thus consistent with a very small $\Delta G^{\ddagger}_v$ for **TMTSF**$^{0/+}$ and $\Delta G^{\ddagger}_s$ values that correlate with $1/r$ but are significantly smaller than predicted by eq 7.[14] The activation limited $\Delta G^{\ddagger}_{ii}$(fit) value for **TMTSF**$^{0/+}$ is only 56% as large as for **TTF**$^{0/+}$ and is heavily dominated (and might be entirely determined) by solvent reorganization. It is striking to note that k_{ii}(fit) of 1.4×10^{11} M^{-1} s^{-1} for **TMTSF**$^{0/+}$ is ca. 10-fold higher than the rate of diffusion at 25 °C in acetonitrile (1.2×10^{10} M^{-1} s^{-1}) and is clearly beyond the scope of any direct method. Nonetheless, the approach described here allows a relatively precise estimate of $\Delta G^{\ddagger}_{ii}$ for **TMTSF**$^{0/+}$ through its cross reactions because its contribution to the cross reaction activation free energy can be readily assessed when the other contributing factors are known. A substantially smaller ΔG_v for **TMTSF**$^{0/+}$ than for **TTF**$^{0/+}$ should be involved in determining the rather different conductivity properties of salts of these compounds and their derivatives, in addition to the overlap effects that have predominated discussions of these differences.[15]

We note that this analysis estimates the ET barrier for **TMPD**$^{0/+}$ to be about 59−44% internal geometry reorganization, but for **TTF**$^{0/+}$ to be less than 33% internal geometry reorganization. Dominate solvent reorganization for **TTF**$^{0/+}$ self-ET is required for the substantial solvent friction effect observed,[7] and dominant internal reorganization is consistent with the lack of such an effect for **TMPD**$^{0/+}$. The larger $\Delta G^{\ddagger}_{ii}$(fit) couples are predicted to have even larger internal geometry reorganization components, 85−90% of the total activation barrier for the largest barrier acyclic hydrazines.

Examining $\Delta G^{\ddagger}_v$(fit) values as we did above implicitly assumes that the V values for the aromatic compounds are similar or rather large. The shallow dependence of ΔG^* on V at high values of V would make changes in V undetectable in our data until it dropped significantly below 0.5 kcal/mol, but the presence of low V value couples should be signaled by failure of consistent apportioning of solvent and internal reorganization effects using the above procedure. As pointed out previously,[5] the most surprising result is that adding bulky alkyl groups in the **TMPD**$^{0/+}$ → **33)$_2$PD**$^{0/+}$ comparison slightly lowers $\Delta G^{\ddagger}_{ii}$(fit) instead of raising it, as would be expected if V were significantly smaller with the bulky alkyl groups. While a slightly smaller $\Delta G^{\ddagger}_s$ resulting from the larger r for **33)$_2$PD**$^{0/+}$ would contribute to lowering $\Delta G^{\ddagger}_{ii}$(fit), the similar $\Delta G^{\ddagger}_{ii}$(fit) values require that V is not much smaller for **33)$_2$PD**$^{0/+}$ than for **TMPD**$^{0/+}$. For example, a decrease of V by a factor of 2 at $V = 0.5$ kcal/mol (holding the other parameters constant) would give an increase in $\Delta G^{\ddagger}_{ii}$(fit) of 1.0 kcal/mol using eq 5. The similar k_{ii}(fit) values for these compounds therefore imply that the effective V value for **33)$_2$PD**$^{0/+}$, which appears to require mostly nonbonded alkyl−alkyl contacts, is not significantly smaller than that for **TMPD**$^{0/+}$. This is a surprising result since **TMPD**$^{0/+}$ ET could occur through a significantly closer approach[7] of the ring π-systems, with the transition state having π-stacked aromatic rings resembling the contact found in crystals. Such an ET transition state for **TMPD**$^{0/+}$ has been suggested by Grampp and Jaenicke.[7] The large alkyl groups of **33)$_2$PD**$^{0/+}$ preclude close approach of the aryl rings, and lead to a significant increase in the inter-ring distance in crystals.[5] Any enhancement of V by ring π system overlap for **TMPD**$^{0/+}$ in the reactions studied apparently does not cause a significant increase in k_{ii}(fit) over that through the alkyl groups of **33)$_2$PD**$^{0/+}$. It must be emphasized that the reactions on which these conclusions are based are with hindered compounds, and that the effective V for self-ET of **TMPD**$^{0/+}$ might be significantly less. Such an effect of larger V for self-ET than for ET with partners having more steric hindrance appears to be observed. $\Delta G^{\ddagger}_{ii}$(fit) − $\Delta G^{\ddagger}_{ii}$(MR) for **TMPD**$^{0/+}$ is the largest measured in the series we have studied,[5] 1.5 kcal/mol. Using eq 6 with $h\nu_v = 1500$ cm^{-1} and keeping λ the same, an increase in k_{ii} from the 1.3×10^8 M^{-1} s^{-1} obtained from the cross rate study to the 1.5×10^9 found by ESR under self-ET conditions[7] corresponds to an increase in V from 0.5 to 1.2 kcal/mol (or from 0.1 to 0.29 kcal/mol, or from 0.05 to 0.15 kcal/mol). An increase in V of this magnitude for changing from a sterically hindered to an unhindered ET partner seems entirely reasonable to us. Equation 2 effectively averages the preexponential factors in calculating k_{ii}, but a plot of preexponential factor versus V using eq 5 is very nonlinear. It may be that using the average of the preexponental factors for a reaction of a high V and a low V component is not the best assumption possible, but eq 2 estimates the observed k_{ij} values well, so the reactions studied apparently do not include examples for which this assumption becomes very poor.

The 0.9 kcal/mol larger $\Delta G^{\ddagger}_{ii}$(fit) for **k33)$_2$PD**$^{0/+}$ than for the very similar **33)$_2$PD**$^{0/+}$ appears to us to be most likely attributable to an effectively smaller V value.[5] It might be clearer to express this effect as representing a smaller fraction of the relative orientations of **k33)$_2$PD**$^{0/+}$ pairs having V as large as that of **33)$_2$PD**$^{0/+}$. Such an "effective cone angle" rationalization has been used in considering effective V values for protein-bound redox centers.[2] A decrease of effective PRE upon each keto-for-CH_2 substitution by a factor of 2 would cause the rate constant change observed if the other ET parameters were the same, as we expect them to be for **33)$_2$PD**$^{0/+}$ and **k33)$_2$PD**$^{0/+}$.

Ferrocenes. The ferrocenes show about 1.5−1.8 kcal/mol larger $\Delta G^{\ddagger}_{ii}$(fit) values than **TMPD**$^{0/+}$ and **33)$_2$PD**$^{0/+}$. The

(14) Much poorer correlation is found for our data using PM3 ΔH_v calculations, which get a significant value for **TMTSF**$^{0/+}$ and reverse the sizes of ΔH_v for **TMPD**$^{0/+}$ and **33)$_2$PD**$^{0/+}$, so smaller $\Delta G^{\ddagger}_s$ as r increases is not obtained.

(15) (a) Williams, J. M.; Wang, H. H.; Emge, T. J.; Geiser, U.; Beno, M.; Leung, P. C. W.; Carlson, K. D.; Thorn, R. J.; Schultz, A. J.; Whangbo, M.-H *Prog. Inorg. Chem.* **1987**, *35*, 51. (b) Wudl, F. *Acc. Chem. Res.* **1984**, *17*, 227.

radius estimated for ferrocene is 3.07 Å, so ΔG_s should not be very much larger than for **TMPD**$^{0/+}$. Either ferrocene $\Delta G^{\ddagger}_v$ values are very much larger than anyone has assumed, or some special effect is raising $\Delta G^{\ddagger}_{ii}$(fit) for ferrocenes relative to **PD** derivatives. Weaver and co-workers pointed out that ferrocenes have a small ΔG_v, assigned essentially all of the ΔG^* they used for **FeCp$_2$**$^{0/+}$ (5.35 kcal/mol in acetonitrile, obtained from the optical spectrum of a dimeric radical cation) as ΔG^*_s, and concluded from a detailed solvent study that V was 0.1 kcal/mol for **FeCp$_2$**$^{0/+}$.[10a,b] A value about this size has also been calculated by Newton and co-workers.[16] Smaller V for **FeCp$_2$**$^{0/+}$ than for aromatic couples may be qualitatively predicted on structural grounds, because V is determined by orbital overlaps of the ET partners. Most of the spin density is at iron in **FeCp$_2$**$^{+}$ (a total π spin density of 0.17 electron on both rings is obtained from the NMR spectrum),[17] but overlap with the iron atom is clearly not necessary to achieve ET. **FeCp*$_2$**$^{0/+}$ certainly has far more hindered approach to its iron atom than ferrocene but has larger k_{ii}(fit) and k_{ii}.[10a,b] Only a small fraction of the spin density thus contributes to overlap with an ET partner for a ferrocene, which makes a smaller V value than for **TMPD**$^{0/+}$ seem reasonable. The intrinsic barriers are also consistent with substantially smaller V values for ferrocenes than for **PD** derivatives. As shown in Figure 3, for ΔG^*(fit) to be smaller for **FeCp$_2$**$^{0/+}$ than for **TMPD**$^{0/+}$, as required if ΔG^*_v is small and ΔG^*_s is not anomalously large, V must be considerably smaller for **FeCp$_2$**$^{0/+}$ than for **TMPD**$^{0/+}$.

Acyclic Hydrazines. Neutral acyclic hydrazines have θ near 90°, and unless nonbonded steric interactions become too large, nearly coplanar lone pair axes in the radical cations. The large θ change between the two oxidation states makes λ_v especially large for such compounds, and the **iPr$_2$N)$_2$**$^{0/+}$ ET is so slow it can be measured by following the ET-mediated scrambling of a deuterium label.[5] We can add nothing to our previous discussion of higher reactivity of **cHx$_2$N)$_2$**$^{0/+}$ than **iPr$_2$N)$_2$**$^{0/+}$.[5] The $\Delta G^{\ddagger}_{ii}$(fit) values for the tetra-*n*-alkylhydrazines **Et$_2$N)$_2$**$^{0/+}$, **nPr$_2$N)$_2$**$^{0/+}$, and **nHx$_2$N)$_2$**$^{0/+}$ are very similar (21.3−21.8 kcal/mol) and slightly larger than that for **iPr$_2$N)$_2$**$^{0/+}$. This seems reasonable because the α-branched alkyl groups of **iPr$_2$N)$_2$**$^{0/+}$ flatten the nitrogens of the neutral form a small amount, making the geometry change upon electron loss slightly smaller than for the *n*-alkyl compounds.[18] The tetra-*n*-alkylhydrazines presumably have very similar ΔG_v and $h\nu_v$ parameters, and their $\Delta G^{\ddagger}_s$ values should only differ slightly as r increases (about 0.7 kcal/mol between the ethyl- and hexyl-substituted compounds assuming an r^{-1} dependence). These facts require that V is nearly constant for the tetra-*n*-alkylhydrazines as well. Because V is not changing significantly for *n*-alkyl group homologation and a barrier drop occurs upon introducing four α-branched substitutents, it appears clear that direct overlap of the two-atom NN π systems is not required for ET in these compounds. Although it might be argued that *n*-alkyl groups could be rotated to allow direct NN π overlap, it seems unlikely that isopropyl groups could be so rotated without an unreasonable increase in nonbonding steric interaction. A similar conclusion of no direct NN overlap was reached using k_{ii} measurements for bis-N,N′-bicyclic hydrazines.[19] Introducing an endo β-phenyl group which prevents close approach of the nitrogen units of **22/u22**$^{0/+}$ caused k_{ii} to drop about a factor of 2. This result shows that transition state geometries which have large direct NN $\pi-\pi$ overlap do not dominate the observed rate constant, and suggests that approaches which place a phenyl group between the hydrazines are ineffective relative to those which do not. Collectively, these observations support the conclusion that direct NN $\pi-\pi$ overlap is not the dominant mechanism of ET for these compounds.

The $\Delta G^{\ddagger}_{ii}$(fit) for **Me$_2$N)$_2$**$^{0/+}$ is 4.5 kcal/mol smaller (k_{ii}(fit) is 2500× larger) than that for **Et$_2$N)$_2$**$^{0/+}$. This is a large effect, in the direction opposite that of the expected λ_s effect (estimated $\Delta G^{\ddagger}_s$ is 0.5 kcal/mol larger for the smaller r **Me$_2$N)$_2$**$^{0/+}$). Moreover, ΔG_v should be slightly larger for **Me$_2$N)$_2$**0/+ than for the *n*-alkyl series because the methyl groups cause less flattening at nitrogen in the neutral compound and the radical cations are all nearly planar at nitrogen.[18] Consequently, the most likely explanation for the lower $\Delta G^{\ddagger}_{ii}$ is a significantly larger V for **Me$_2$N)$_2$**$^{0/+}$, which can achieve closer approach of the ET partners. Molecular modeling indicates that there is clearly greater exposure of the HOMO in the vicinity of the nitrogen atoms to solvent or an ET partner for both oxidation states of **Me$_2$N)$_2$** than for *n*-alkyl compounds. Even replacing two methyl groups by isopropyl groups increases $\Delta G^{\ddagger}_{ii}$ by 2.9 kcal/mol (for **iPrMeN)$_2$**$^{0/+}$) and 3.4 kcal/mol (for **iPr$_2$NNMe$_2$**$^{0/+}$). Having even two α-branched alkyl groups eliminates most (but not all) of the barrier-lowering effect observed for **Me$_2$N)$_2$**$^{0/+}$, which seems consistent with our attribution of it to a direct two-atom π system overlap effect, which should be quite sensitive to steric effects. Even when both isopropyl groups are attached to one nitrogen, nonbonded steric effects force one isopropyl group to have its methyl groups directed back toward the other nitrogen, apparently effectively shielding both nitrogens from direct overlap with an approaching ET partner. We noted above that a similar rate increase was not observed for decreasing alkyl group size in the eight-atom π system **PD** derivatives. The larger π amine system considerably disperses charge compared to the two-atom π system of hydrazines, which might make such an effect much smaller.

Comparison of $\Delta G^{\ddagger}_{ii}$(fit) Values with Optically Derived λ Values. Experimental λ values that are independent of ET rate constant measurements are available from the optical spectra of charge-localized symmetrical intervalence compounds. They have a bridge connecting the same charge-bearing units, each of which can be present in either the neutral or radical cation oxidation state. When the bridge provides large enough V, an intervalence compound shows a charge-transfer band that has a transition energy at the band maximum (E_{op}) equal to Marcus's λ using Marcus−Hush theory.[2] We shall call λ estimated in this way λ(opt) to distinguish it from other estimates of λ. Optical data are available for examples having **22/tBuMe**,[8a] **22/tBuiPr**,[8c] and **22/22**[8b] charge-bearing units connected by two four-σ-bond pathways linking pairs of nitrogens, and also for a *p*-phenylene bishydrazine that has **22/tBuPh** charge-bearing units[8d,e] (see Table 4and structures in Scheme 3). Because λ_s values for intra- and intermolecular ET will be different, it is necessary to separate solvent and internal vibrational reorganization terms for meaningful comparison of the barriers. Precise separation of λ_s and λ_v from optical data on intervalence compounds is problematic. Although vibronic coupling theory simulation of the optical transition band shape has been

(16) Newton, M. D.; Ohta, K.; Zhang, E. *J. Phys. Chem.* **1991**, *95*, 2317.

(17) Nelsen, S. F.; Chen, L.-J.; Ramm, M. T.; Voy, G. T.; Powell, D. R.; Accola, M. A.; Seehafer, T.; Sabelko, J.; and Pladziewicz; J. R. *J. Org. Chem.* **1996**, *61*, 1405.

(18) We note the AM1-calculated ΔH_v value for **Et$_2$N)$_2$**$^{0/+}$ quoted in Table 1 does not agree with this expectation that ΔG^*_v should be larger for *n*-alkyl groups than for branched alkyl groups. It is not obvious that we have obtained ΔH_v properly, because the value calculated is expected to be very sensitive to alkyl group conformations. A larger ΔH_v is calculated for **Me$_2$N)$_2$**$^{0/+}$, as expected, but the change between the methyl and ethyl compounds appears likely to be overestimated.

(19) Nelsen, S. F.; Wang, Y.; Hiyashi, R. K.; Powell, D. R.; Neugebauer, F. A. *J. Org. Chem.* **1995**, *60*, 2981.

Table 4. Comparison of λ Derived from Optical Data on Intervalence Bishydrazines with Barriers for Self-ET of the Charge-Bearing Units

intervalence compound	$E_{op} = \lambda$(opt), kcal/mol	rel λ_s	estimated ΔG^*_v(opt)[a]	hydrazine	estimated $\Delta G^{\ddagger}_v$(fit)[b]
BMT$^+$	55.8	0.91	11.9	**22/tBuMe**$^{0/+}$	13.4(5)
BMH$^+$	52.2	0.98	10.9		
BIT$^+$	51.6	0.76	11.2	**22/tBuiPr**$^{0/+}$	14.0(5)
BIH$^+$	48.6	0.83	10.3		
22H$^+$	46.6	1.00	9.4	**22/22**$^{0/+}$	12.7(5)
H$_4$ $^+$	37.2	0.96	7.2	**22/tBuPh**$^{0/+}$	11.6(5)

[a] Units, kcal/mol. Assuming ΔG^*_s(opt) = 9 kcal/mol (see the text). [b] Units, kcal/mol. Range quoted uses $\Delta G^{\ddagger}_v$(**TMTSF**$^{0/+}$) in the range 0−1 kcal/mol and assumes r^{-1} dependence of $\Delta G^{\ddagger}_s$.

Scheme 3. Dimeric Hydrazines

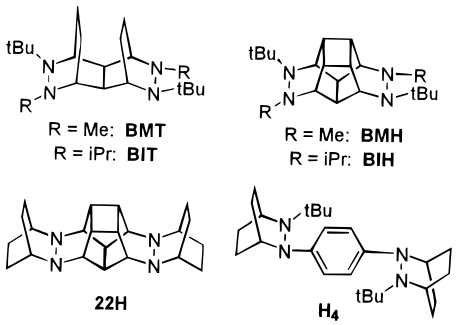

attempted, serious problems were noted in trying to do such a separation.[8c,e] Using vibronic coupling theory, the λ values obtained are significantly higher than E_{op}, so λ no longer has the Marcus−Hush definition of being the vertical energy gap between the ground-state surface and the excited-state surface. The λ_s, λ_v partitioning obtained is so sensitive to the $h\nu_v$ employed that almost any ratio will fit the band equally well if $h\nu_v$ is considered to be a variable in fitting the band.[8c,e] The traditional way of separating λ_s from λ_v for an intervalence compound is to plot E_{op} versus γ and use the intercept as λ_v.[2] Such a plot is linear for **22H**$^+$,[8b] and gives $\lambda_s(CH_3CN) = 9.0$ kcal/mol.[8c] Table 4 uses the crude estimate of the distance factor for an intervalence compound, being $g(r,d) = r_{av}^{-1} - d^{-1}$, where d is the distance between the charge-bearing centers, using X-ray crystallographic N−N distances for d values, to scale λ_s for each compound: λ_s(est)[**x**] = 9.0[$g(r,d)$[**x**]/$g(r,d)$[**22H**$^+$]. This distance factor is consistent with the E_{op} versus γ plot for **22H**$^+$.[8b] This approach attempts to account for the larger charge-bearing unit of **22/tBuiPr** and **22/tBuPh** versus **22/tBuMe** and **22/22** (see Table 1), and the fact that d is larger for hexacyclic saturated bridged compounds than for tetracyclic bridged ones (5.03 and 4.86 Å, respectively). The use of d = 5.66 Å for **H$_4$**$^+$ is discussed elsewhere.[6e] While the ΔG^*_v(opt) = [$\lambda - \lambda_s$(est)]/4 values in Table 4 may be of limited accuracy,[20] it is not clear how to improve them. The structure of the bridge as well as the charge-bearing units affects λ(opt). Smaller λ(opt) occurs for hexacyclic- than for tetracyclic-bridged compounds having both **22/tBuMe** and **22/tBuiPr** charge-bearing units. This is attributed to less twisting in the central portion of the molecule when the hexacyclic bridge is present, because λ_v is clearly very sensitive to the geometry of the charge-bearing units.[8a,c] It will be noted that **BMT**$^+$ and **BMH**$^+$ have higher $\Delta G^{\ddagger}_v$(opt) values than **BIT**$^+$ and **BIH**$^+$, as expected, because replacing methyl by isopropyl significantly flattens the nitrogen in these compounds,[21] which is known to lower λ_v.

Table 4 also shows $\Delta G^{\ddagger}_v$(fit) values for the hydrazine couples used as charge-bearing units in the intervalence compounds. They are estimated using $\Delta G^{\ddagger}_{ii}$(fit) = $\Delta G^{\ddagger}_v$(fit) + $\Delta G^{\ddagger}_s$, using $\Delta G^{\ddagger}_s$(**TMTSF**$^{0/+}$) = 2.3−1.3 kcal/mol and assuming r^{-1} dependence of $\Delta G^{\ddagger}_s$ values. Despite significant uncertainty in the separation of solvent and internal vibrational reorganizational energy effects for both the optical barriers and those measured in cross rate studies, it is clear that $\Delta G^{\ddagger}_v$(fit) is larger than ΔG^*_v(opt). The small V values for intermolecular ET reactions involving tetra-α-branched hydrazines obtained above from the significantly smaller $\Delta G^{\ddagger}_{ii}$(fit) for **Me$_2$N)$_2$**$^{0/+}$ require that ΔG^*_{ii}(fit) will be significantly smaller than $\Delta G^{\ddagger}_{ii}$(fit), so these results are consistent with expectation. The $\Delta G^{\ddagger}_v$(fit) − ΔG^*_v(opt) differences cannot be interpreted very quantitatively because it is not clear that the correct ΔG^*_s(opt) values were employed; they all rest on the assumption that it is 9 kcal/mol for **22H**$^+$.

In contrast to optical data for dimeric radical cations, $\Delta G^{\ddagger}_{ii}$(fit) for **22/tBuMe**$^{0/+}$ is 0.5 kcal/mol smaller than that for **22/tBuiPr**$^{0/+}$ (Table 1), and trying to allow for $\Delta G^{\ddagger}_s$ effects in comparing $\Delta G^{\ddagger}_v$ values gives a 0.6 kcal/mol difference (Table 4). We conclude that some other factor is important enough to reverse the reactivity order expected for these two compounds from the vertical internal reorganization energies for their related intervalence compounds. It seems possible that a small direct overlap enhancement of V is still present for the bimolecular ET when only one methyl group is present at nitrogen.

Diamine N[333]N. The diamine **N[333]N**$^{0/+}$ ET has an intrinsic ET barrier between those of the $\theta \approx 120°$ hydrazines **22/tBuMe**$^{0/+}$ and **22/tBuiPr**$^{0/+}$. This demonstrates that λ_v is substantial for this diamine system, approaching the middle of the range for hydrazines. We presume that its tetramethylene-bridged analogue, which has an even larger geometry change upon electron removal,[7] would show even slower ET. We have not been able to study simple amines, which have far smaller vertical reorganization energies, because their k_{ij} values are too large to measure using the couples of Table 1.

Conclusions

Stopped-flow cross reaction studies allow obtaining activation-limited k_{ii}(fit) values for low barrier aromatic compounds (their k_{ii} values are not activation limited), for hydrazines with relatively unstable radical cations, and for hydrazines and a diamine having values too small to measure by line broadening methods. This allowed estimation of k_{ii} for 18 compounds for which no direct measurement presently exists, and extends the range for intrinsic ET rate constants studied to 2×10^{14}. The series of compounds studied here ranges from **TMTSF**$^{0/+}$, for which the ET barrier originates mostly from solvent reorganization, to acyclic hydrazines, for which it originates ≥90% from bond reorganization, and the couples studied have a wide range of $h\nu_v$ and steric hindrance. The relative invariance of $\Delta G^{\ddagger}_{ii}$(fit) for compounds common to the earlier 47 reaction database and that including the additional 44 reactions reported here gives us confidence that the approach described is effective at

(20) Dielectric continuum theory only works well for describing solvent effects on E_{op} for **22H**$^+$ among the dimeric hydrazines of Scheme 3. Ion pairing effects, which will be discussed in the future, occur in less polar solvents. We have no evidence for significant ion pairing of any of these compounds in acetonitrile.

(21) Nelsen, S. F.; Ramm, M. T.; Wolff, J. J.; Powell, D. R. *J. Org. Chem.* **1996**, *61*, 4703.

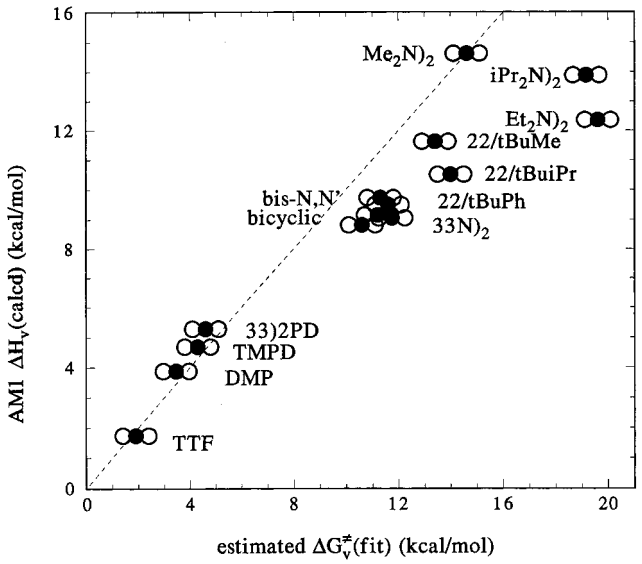

Figure 5. AM1 ΔH_v(calcd) versus estimated $\Delta G^{\ddagger}_v = \Delta G^{\ddagger}_{ii}(\text{fit}) - \Delta G^{\ddagger}_s$ for aromatics and hydrazines.[17] Three points are plotted for each couple, those obtained using $\Delta G^{\ddagger}_v(\mathbf{TMTSF}^{0/+}) = 0$, 1, and their average (shown as the filled circle). The dotted line has a slope of 1.

obtaining useful $\Delta G^{\ddagger}_{ii}$ values. Figure 1 most clearly shows the predictive value of the resulting $\Delta G^{\ddagger}_{ii}$(fit) for the 31 compounds studied.

The $\Delta G^{\ddagger}_{ii}$(fit) values for aromatic compounds are smaller than ΔG_s values calculated using Marcus's familiar dielectric continuum formula, but when values of $\Delta G^{\ddagger}_s$ scaled to experimental values (using $\Delta G^{\ddagger}_s(\mathbf{TMTSF}^{0/+}) = \Delta G^{\ddagger}_{ii}(\mathbf{TMTSF}^{0/+})$), and are estimated assuming the r^{-1} dependence it predicts, a plot of $\Delta G^{\ddagger}_v(\text{inter}) = \Delta G^{\ddagger}_{ii}(\text{fit}) - \Delta G^{\ddagger}_s(\text{est})$ versus AM1-calculated vertical reorganization enthalpy is linear, suggesting that variations in V do not very much affect the >4 kcal/mol range in $\Delta G^{\ddagger}_{ii}$(fit) for these aromatic compounds. However, because Marcus's cross reaction eq 2 assumes constant preexponential factors, effects of variations of V between the couples must be incorporated into the k_{ii}(fit) values obtained. $\Delta G^{\ddagger}_{ii}$(fit) values should be larger than $\Delta G^{\ddagger}_{ii}$ values determined under self-exchange conditions unless V for the cross reaction is as large on average as for the related self-exchanges, and ΔG^{*}_{ii}(fit) becomes increasingly smaller than $\Delta G^{\ddagger}_{ii}$(fit) as V for the cross reaction drops. When a larger range of structural variation is considered, such effects are clearly present. A smaller V appears principally responsible for the smaller k_{ii}(fit) values for ferrocenes than for $\mathbf{TMPD}^{0/+}$, and that the 2500-fold higher reactivity of $\mathbf{Me_2N)_2}^{0/+}$ than $\mathbf{Et_2N)_2}^{0/+}$ originates from a larger V for $\mathbf{Me_2N)_2}^{0/+}$, resulting from smaller steric interactions allowing direct NN, π system overlap with an ET partner, which apparently does not occur significantly even for *n*-alkylhydrazines. A plot of ΔH_v(calcd) versus estimated $\Delta G^{\ddagger}_v$(fit) values ($\Delta G^{\ddagger}_{ii}$(fit) values "corrected" using r values to allow for λ_s effects) is shown as Figure 5;[22] the dashed line shows a slope of 1. It is not clear how accurate the ΔH_v values are, but larger $\Delta G^{\ddagger}_v$ values for the more hindered hydrazines than $\mathbf{Me_2N)_2}^{0/+}$ probably result at least partially from smaller V values for the more hindered compounds.

(22) The bis-N,N′-bicyclic hydrazines are **21/21**, **22/u22**, and **21/u22**, which are untwisted in both oxidation states. AM1 calculations underestimate λ'_v for $\mathbf{22/22}^{0/+}$ relative to bis-N,N′-bicyclic systems which are not twisted in the neutral form because they incorrectly determine **22/22**° to be untwisted.[6] A point for $\mathbf{22/22}^{0/+}$ was therefore omitted. Both the $\mathbf{33)_2PD}$ and $\mathbf{33N)_2}$ calculations are not for the AM1 energy minima but for neutral compound twist angles which are independently known to be realistic.

Experimental Section

TTF, **TMTSF**, and **DMP** were obtained from Aldrich and used as received. Solutions of $\mathbf{TMTSF}^+$ and $\mathbf{TTF}^+$ for kinetic studies were prepared by 1 equiv oxidation of **TMTSF** and **TTF** by $NOPF_6$ in acetonitrile. Solutions of $\mathbf{DMP}^+$ were prepared by 1 equiv oxidation of **DMP** by $\mathbf{FeCp'_2PF_6}$ in acetonitrile. The syntheses of **22/tBuMe**,[24a] **22/iPr2**,[24b] **22/tBuiPr**,[24b] **22/tBuPh**,[24c] **iPrMeN)2**,[24d] **iPr2NNMe2**,[24d] **N[333]N**,[17] and their related radical cation salts used in this work have been described elsewhere. **Me2N)2** (Fluka) was purified by GC.

Et2N)2, **nPr2N)2**, and **nHx2N)2** were prepared by a common method; the details for **Et2N)2** are given here. A distinct advantage of this methods is that it avoids the use of *N*-nitrosoamines, previously used in these syntheses, which are carcinogenic and mutagenic. [**Caution**: tetraethylhydrazine is extremely volatile!] Bromoethane (15.2 mL, 201 mmol) was slowly added dropwise at room temperature through a condenser to a stirring solution of hydrazine monohydrate (9.7 mL, 200 mmol) and absolute ethanol (10 mL) during which it refluxed without additional heat. Heat was then applied to maintain gentle reflux for an additional hour. The solution was allowed to cool overnight with stirring. A NaOH solution (10.010 g, 0.25 mol, in 30 mL of H_2O) was added to dissolve the hydrazine salts. The solution was extracted with pentane (2 × 20 mL), washed with a saturated NaCl solution, dried over $MgSO_4$, and evaporated to yield a mixture of mono-, di-, and triethylhydrazine (0.222 g). The aqueous layer was saturated with solid NaCl, extracted with ether (2 × 20 mL), dried over $MgSO_4$, and evaporated to yield an additional mixture of mono-, di-, and triethylhydrazine (4.748 g). Acetaldehyde (7.8 mL, 139.7 mmol), while being kept at a temperature below 0 °C, was added dropwise under nitrogen to a stirring mixture of mono-, di-, and triethylhydrazine in ether (4.970 g obtained in the previous reaction) and acetonitrile (100 mL). Upon completion, $NaBH_3CN$ (2.941 g, 44.5 mmol) was added and stirred. Acetic acid (5.4 mL, 93.6 mmol) was added in small amounts over a period of 45 min, and the solution was stirred overnight under nitrogen at room temperature. Concentrated HCl (9 mL, 37.5%) was then added until the solution became acidic and gases no longer evolved.. Upon evaporation of the acetonitrile, a NaOH solution (9.919 g, 25.0 mmol, in 30 mL of H_2O) was slowly added, while the mixture was cooled in a room-temperature water bath, until the solution became basic. A saturated NaCl solution (30 mL) was then added with stirring to the basic solution. The reaction mixture was extracted with ether (3 × 20 mL) and dried over $MgSO_4$. The ether was removed by distillation (760 mmHg, 45 °C) to yield tetraethylhydrazine (4.50 g). A sample (2.998 g, 20.8 mmol) of crude tetraethylhydrazine was filtered through 100 g of silica gel (2% ether in pentane, $R_f = 0.39$) and evaporated in several fractions to yield tetraethylhydrazine. Traces of the ether were removed by distillation (760 mmHg, 45 °C) through a vacuum-jacketed 30 cm Vigreux column to yield pure tetraethylhydrazine as a slightly yellow oil (0.752 g, 5.22 mmol). ^{1}H NMR (300 MHz, $CDCl_3$): δ 2.460 (q, 2H), 1.024 (t, 3H).

The cyclic voltammetry and stopped-flow experiments were conducted as previously described.[5] The $E^{\circ\prime}$ values for $\mathbf{TMTSF}^{0/+}$ and $\mathbf{TTF}^{0/+}$ require special comment because literature values vary so much with solvent and who reported them. For example, values in methylene chloride have been reported at 0.54 V ($\mathbf{TMTSF}^{0/+}$)[23a] and $\Delta E^{\circ\prime} = E^{\circ\prime}(\mathbf{TMTSF}^{0/+}) - E^{\circ\prime}(\mathbf{TTF}^{0/+}) = 0.167$,[23b] but more recently at 0.53 and 0.52 V, respectively ($\Delta E^{\circ\prime} = 0.01$),[23c] and in benzonitrile values of 0.42 and 0.24 V ($\Delta E^{\circ\prime} = 0.18$),[23d] and 0.47 and 0.40 V ($\Delta E^{\circ\prime} = 0.07$)[23c] have been reported. $E^{\circ\prime}$ values are strongly affected by ion pairing in nonpolar solvents, which probably contributes to the problems in internal consistency for the literature values. We have not found

(23) (a) Lerstrup, K.; Toulham, D.; Bloch, A.; Poeler, T. Cowan, D. *J. Chem. Soc., Chem. Commun.* **1982**, 336. (b) Bechgaard, K.; Cowan, D. O.; Bloch, A. N. *J. Chem. Soc., Chem. Commun.* **1974**, 937. (c) Zambounis, J. S.; Christen, E.; Pfeiffer, J.; Rihs, G. *J. Am. Chem. Soc.* **1994**, *116*, 925. (d) Wudl, F.; Aharon-Shalom, E. *J. Am. Chem. Soc.* **1982**, *104*, 1154.

(24) (a) Nelsen, S. F.; Wolff, J. J.; Chang, H.; Powell, D. R. *J. Am. Chem. Soc.* **1991**, *113*, 7882. (b) Nelsen, S. F.; Chen, L.-J.; Petillo, P. A.; Evans, D. H.; Neugebauer, F. A. *J. Am. Chem. Soc.* **1993**, *115*, 10611. (c) Nelsen, S. F.; Ismagilov, R. F.; Powell, D. R. *J. Am. Chem. Soc.* **1996**, *118*, 6313. (d) Nelsen, S. F.; Peacock, V.; Weisman, G. R. *J. Am. Chem. Soc.* **1976**, *98*, 5269.

literature values in a polar solvent, where ion pairing effects should be less important. We determined the values in acetonitrile containing 0.1 M tetrabutylammonium perchlorate, the solvent in which we need to know $E^{\circ\prime}$ accurately for this work. We found that **TMTSF**^{0} is rather insoluble in acetonitrile and that an anomalous wave shape was observed for the first oxidation wave. However, **TMTSF**$^+$ reduction was well behaved, as was **TTF**^{0} oxidation, and gave the values quoted in Table 1. We also confirmed the approximate correctness of the **TMTSF**$^{0/+}$ potential with equilibrium spectrophotometric measurements on the reaction of **TMTSF**^{0} with **k33N)$_2$**$^+$.

Acknowledgment. We thank the National Science Foundation for partial financial support of this work under Grants CHE-9504133 (J.R.P.) and CHE-9417946 (S.F.N.). Acknowledgment is also make to the donors of the Petroleum Research Fund, administered by the American Chemical Society, for partial support of the research under Grant ACS-PRF 29982-B4 (J.R.P.).

JA9810890